American Mineralogist, Volume 76, pages 92–99, 1991

Structures of low gallium albite ($NaGaSi_3O_8$) and intermediate germanium albite ($NaAlGe_3O_8$): Tetrahedral-site ordering in sodium feldspar

MICHAEL E. FLEET
Department of Geology, University of Western Ontario, London, Ontario N6A 5B7, Canada

ABSTRACT

The structure of low gallium albite ($NaGaSi_3O_8$), synthesized hydrothermally at 600 °C and 1.3 kbar, has been refined at room temperature with single-crystal X-ray intensities to $R = 0.023$. Mean T-O bond distances and Ga site occupancies are: T_10 [1.807(2), 0.935(1)], T_1m [1.610(2), 0.016(1)], T_20 [1.615(2), 0.025(1)], T_2m [1.619(2) Å, 0.025(1)]. The structure of intermediate germanium albite ($NaAlGe_3O_8$), grown with a vanadotungstate flux, has been refined similarly to $R = 0.026$. Mean T-O bond lengths and Al site occupancies are: T_10 [1.737(2), 0.274(2)], T_1m [1.728(3), 0.375(2)], T_20 [1.736(2), 0.185(2)], T_2m [1.735(2) Å, 0.166(2)]. Tetrahedral-site ordering in strain-free sodium silicate feldspar structures is promoted by the distinctive stereochemistries of the T_10 and T_1m sites, which are imposed by spatial accommodation of the Na cation within the feldspar framework. From site occupancies for Si, Al, Ga, Ge, B, and Fe^{3+}, it is tentatively concluded that the ordering scheme is determined by the favorable charge or valence electron distribution resulting when the trivalent atom is placed in the T_10 site, and that this site preference is proportional to the difference in size of the trivalent and quadrivalent atoms. Electrostatic repulsion between the T and Na atoms may be a contributing factor. Intermediate germanium albite has $(t_10 + t_1m) > (t_20 + t_2m)$, as in intermediate microcline and low sanidine, but the unusual site preference of $t_1m > t_10 \approx 0.25$ is unexplained.

INTRODUCTION

Study of the crystal structures of alkali feldspars is complicated by sluggishness of Al/Si ordering and small differences in X-ray scattering efficiencies of Al and Si. Earlier work leading to the present understanding of these structures is reviewed in Smith (1974), Ribbe (1983), and Smith and Brown (1988). Structural aspects of albite of continuing interest include change in tetrahedral-site occupancies with progress of the order-disorder transformation (e.g., Burns and Fleet, 1990), nature of structures with intermediate states of order (e.g., Phillips et al., 1989), and relative contributions of time-averaged and space-averaged components to X-ray and neutron structures (e.g., Prewitt et al., 1976; Winter et al., 1977; Harlow and Brown, 1980; Swanson, 1986; Smith et al., 1986).

The structures of triclinic alkali feldspars (space group $C\bar{1}$) have four nonequivalent tetrahedral sites for Si and Al, designated by T_10, T_1m, T_20, and T_2m, with occupancies of Al (or trivalent atoms) designated by t_10, t_1m, t_20, and t_2m, respectively. Natural low albite has an almost ideally ordered distribution of Si and Al with $t_10 \approx 1$ and $t_1m \geq t_20 \approx t_2m \approx 0$ (Wainwright and Starkey, 1968; Harlow and Brown, 1980), whereas high albite, produced experimentally by transformation of natural low albite, has a largely disordered structure with $t_10 > t_1m \approx t_20 \approx t_2m \approx 0.25$ (Ribbe et al., 1969; Wainwright and Starkey, cited in Table 3-2 of Smith, 1974). Intermediate-ordered structure also exists at moderate pressures (Su et al., 1986); a recent structure determination of one of these laboratory-transformed albites gave $t_10 = 0.51$, $t_1m = 0.15$, $t_20 = 0.16$, and $t_2m = 0.17$ (Phillips et al., 1989). Natural K-rich feldspars of monoclinic symmetry have $t_10 = t_1m > t_20 = t_2m$, and of triclinic symmetry have $t_10 > t_1m \geq t_20 \approx t_2m$ (e.g., Kroll and Ribbe, 1983, 1987). Thus, tetrahedral-site ordering paths closely approximate to $t_10 \rightarrow 1$, $t_1m \approx t_20 \approx t_2m \rightarrow 0$ in low albite, and $t_10 \rightarrow 1$, $t_1m \geq t_20 \approx t_2m \rightarrow 0$ in triclinic K-rich feldspars.

Electron density at the Na atom position in both low and high albite is markedly anisotropic, the effect being much larger in the latter. There is an extensive debate on whether this represents true thermal motion or positional disorder of the Na atom. Structures with multiple positions (of partial occupancy) for Na have refined satisfactorily (generally, two half-atom positions in low albite and four quarter-atom positions in high albite; e.g., Prewitt et al., 1976; Winter et al., 1977; Harlow and Brown, 1980). Winter et al. (1977) reported that for low albite from Tiburon, California the thermal motion of the Na atom extrapolates to zero at 0 K, indicating that the anisotropic electron density distribution at the Na position is attributable to a time average of highly anisotropic thermal vibration within the aluminosilicate framework. On the other hand, in high albite it does appear to be largely a space average of multiple positions of partial occupancy, as indicated by the split-atom refinements.

0003–004X/91/0102–0092$02.00

More recently, Smith et al. (1986) have shown that the thermal parameters for Na in low albite from Amelia, Virginia extrapolate to positive values at 0 K; i.e., the Na atom appears to have zero-point energy.

Synthetic end-member Ga-, Fe^{3+}-, and Ge-substituted feldspars have been investigated by Pentinghaus (1970), who reported that only $NaGaSi_3O_8$ (gallium albite) exhibited rapid tetrahedral-site ordering. Swanson (1986) subsequently synthesized a single crystal of gallium albite hydrothermally at 650 °C and 1 kbar, and determined the tetrahedral-site occupancies of Ga to be $t_10 = 0.89$, $t_1m = 0.03$, $t_20 = 0.04$, $t_2m = 0.04$. Very recently, the order-disorder transformation in gallium albite was reversed by dry annealing under a load pressure of approximately 1 kbar and the experimental products investigated using Rietveld structure refinement (Burns and Fleet, 1990). The order-disorder transformation in gallium albite is continuous but exhibits a well-defined region of intermediate structure. The ordering path is $t_10 \rightarrow 1$, $t_1m \approx t_20 \approx t_2m \rightarrow 0$, with some tendency for $t_2m \neq t_20$.

Grunwald (1981) refined the structure of germanium albite synthesized hydrothermally at 600 °C and 1 kbar but did not include tetrahedral-site occupancies. However, Smith and Brown (1988) noted that the mean tetrahedral (T-O) bond distances for this refinement, T_10 (1.734), T_1m (1.728), T_20 (1.756), and T_2m (1.736 Å), indicate that Al is concentrated in T_1m at the expense of T_20.

This paper reports on the X-ray single-crystal structure of ordered (low) gallium albite ($NaGaSi_3O_8$) and incompletely disordered (intermediate) germanium albite ($NaAlGe_3O_8$). Structure analysis is facilitated by the large difference in the X-ray scattering efficiencies of Ga and Si, and Al and Ge, respectively. This permits the direct determination of tetrahedral-site occupanices and yields detailed information on the response of the triclinic feldspar structure to tetrahedral cation substitution.

EXPERIMENTAL PROCEDURES

Gallium albite ($NaGaSi_3O_8$)

Gallium albite crystals were grown from a melt using a standard cold-seal hydrothermal reaction vessel. Starting material of $NaGaSi_3O_8$ composition was in the form of a glass, which was prepared from purified Ga_2O_3 and SiO_2 and analytical grade Na_2CO_3. The charge consisted of 0.10 g gallium albite glass, 0.08 g of Na_2CO_3, and 0.03 cm^3 of deionized H_2O contained in a sealed Au capsule about 5 cm in length. It was heated to 845 °C at 1.4 kbar for 2 h (to achieve complete melting), cooled stepwise and maintained at 640 °C overnight, and then further cooled stepwise and maintained at 600 °C and 1.3 kbar for 6 d, and quenched in air and H_2O. The products consisted of isolated and massive aggregates of larger crystals of gallium albite (up to 0.2 mm in diameter) and fine-grained quench material. All gallium albite crystals in this and similar experiments developed a cleavelandite-like growth habit and mosaic spread was evident in their single crystal X-ray diffraction patterns. The crystal used for measurement of reflection intensities was reduced in size with a scalpel blade until the mosaic spread observed in X-ray precession films was minimal.

The crystal was a flattened trigonal prism in shape, with dimensions of 0.10 × 0.12 × 0.05 mm and a calculated volume of 0.30×10^{-3} mm^3. All single-crystal measurements were made with an Enraf-Nonius CAD-4F diffractometer, using graphite-monochromatized Mo$K\alpha$ X-radiation. The unit-cell parameters [$a = 8.161(2)$, $b = 12.851(2)$, $c = 7.191(1)$ Å, $\alpha = 94.39(1)$, $\beta = 116.52(1)$, $\gamma = 87.38(1)°$, $V = 672.7$ Å^3] were refined from 20 reflections in the 2θ range 33.4–37.2°. Intensity data were collected by ω-scan with a scan angle (ω) = 1.6° and correction for dispersion. A total of 3911 *hkl* reflections allowed by space group $C\bar{1}$ out to $2\theta = 60°$ were measured ($-11 \leq h \leq 11$, $-18 \leq k \leq 18$, $-10 \leq l \leq 10$). Standard reflections were 002, 040, 220 and there was no significant variation in intensity ($R_{int} = 0.02$). Background, Lorentz, polarization and absorption corrections were applied; transmission factors (calculated by Gaussian integration with a 12 × 12 × 12 grid and $\mu = 49.1$ cm^{-1}) varied from 0.722 for $-10,4,4$ to 0.830 for $-1,-1,1$. There were 1956 unique reflections, with 602 considered unobserved on the basis of $I < 3\sigma(I)$ $\{\sigma(I) = [I_m + 0.002^2(I_m - B)^2 + 0.005^2(I - I_m)^2]^{1/2}$, I_m, measured intensity and B, background: the three contributions to $\sigma(I)$ represent the statistical error, a proportional error, and the uncertainty in the absorption correction; see program DATAP77 below}.

The structure refinement proceeded from the positional parameters for high albite (Wainwright, cited in Table 4-1 of Smith, 1974). The function, $\Sigma w(\Delta F)^2$ was minimized ($w = 1/\sigma^2$), and unobserved reflections were given a low weight ($\sigma = 1000$). Refinement in $C\bar{1}$ using all reflections out to $2\theta = 60°$ and 118 variable parameters, converged to $R = 0.023$, $R_w = 0.022$ [for reflections with $I \geq 3\sigma(I)$, $S = 0.776$, $(\Delta/\sigma)_{max} = 2 \times 10^{-6}$, $\Delta\rho = -0.31$ eÅ^{-3} at 0.06,0.16,0.22 (near T_10) to 0.36 eÅ^{-3} at 0.30,0.04,0.11 (near Na)]. The isotropic extinction parameter for type I extinction (g; Coppens and Hamilton, 1970) refined to a negative value close to zero and was therefore set to zero in the final cycles of refinement. Scattering factors for neutral atomic species and f', f'' were taken, respectively, from Tables 2.2B and 2.3.1 of the *International Tables for X-ray Crystallography* (1974). All computations were carried out with DATAP77 and LINEX77 (P. Coppens, State University of New York at Buffalo). Final parameters are given in Tables 1 and 2, and observed and calculated structure factors in Table 3.[1]

Germanium albite ($NaAlGe_3O_8$)

Germanium albite crystals were grown from a vanadotungstate flux using a nutrient of composition Na-

---

[1] A copy of Table 3 may be ordered as Document AM-91-447 from the Business Office, Mineralogical Society of America, 1130 Seventeenth Street NW, Suite 330, Washington, DC 20036, U.S.A. Please remit $5.00 in advance for the microfiche.

TABLE 1. Positional and isotropic thermal parameters (Å²)

$B_{eq} = \frac{4}{3}\Sigma_i\Sigma_j\, \beta_{ij}\, \mathbf{a}_i\cdot\mathbf{a}_j$

	x	y	z	B_{eq}
		Gallium albite ($NaGaSi_3O_8$)		
Na	0.2689(2)	0.9877(1)	0.1484(2)	3.06(3)
$T_1$0	0.00922(5)	0.16994(3)	0.20489(6)	0.72(1)
T_1m	0.0013(1)	0.8197(1)	0.2414(1)	0.62(1)
$T_2$0	0.6929(1)	0.1098(1)	0.3118(1)	0.64(1)
T_2m	0.6782(1)	0.8826(1)	0.3618(1)	0.66(1)
O_A1	0.0092(3)	0.1280(2)	0.9581(3)	1.27(6)
O_A2	0.5921(3)	0.9980(2)	0.2809(3)	0.96(5)
O_B0	0.8082(3)	0.1049(2)	0.1810(3)	1.27(6)
O_Bm	0.8174(3)	0.8454(2)	0.2648(3)	1.44(6)
O_C0	0.0042(3)	0.3072(2)	0.2711(3)	1.18(6)
O_Cm	0.0280(3)	0.6940(2)	0.2288(3)	1.11(6)
O_D0	0.2153(3)	0.1073(2)	0.3878(3)	1.22(6)
O_Dm	0.1779(3)	0.8678(2)	0.4423(3)	1.42(6)
		Germanium albite ($NaAlGe_3O_8$)		
Na	0.2732(3)	0.0187(3)	0.1218(4)	8.23(11)
$T_1$0	0.01066(6)	0.15782(3)	0.21137(7)	0.70(1)
T_1m	0.00205(7)	0.81213(4)	0.22968(8)	0.75(1)
$T_2$0	0.68829(5)	0.10494(3)	0.31238(6)	0.75(1)
T_2m	0.67675(5)	0.87440(3)	0.35631(6)	0.79(1)
O_A1	0.0105(4)	0.1281(2)	0.9783(4)	1.47(6)
O_A2	0.5758(3)	0.9865(2)	0.2713(4)	0.96(5)
O_B0	0.8202(3)	0.0920(2)	0.1839(4)	1.64(6)
O_Bm	0.8080(4)	0.8363(2)	0.2443(5)	2.34(7)
O_C0	0.0033(3)	0.2837(2)	0.2875(4)	1.27(5)
O_Cm	0.0152(3)	0.6822(2)	0.1971(4)	1.44(6)
O_D0	0.2042(3)	0.1058(2)	0.3795(4)	1.46(6)
O_Dm	0.1914(4)	0.8645(2)	0.4323(4)	2.09(7)

TABLE 2. Anisotropic thermal parameters (×10² Å²)

	B_{11}	B_{22}	B_{33}	B_{12}	B_{13}	B_{23}
			Gallium albite ($NaGaSi_3O_8$)			
Na	153(7)	436(8)	276(7)	−59(6)	79(6)	−219(6)
$T_1$0	92(2)	69(1)	56(1)	−21(1)	34(1)	−1(1)
T_1m	78(3)	61(3)	48(3)	−1(3)	30(3)	5(3)
$T_2$0	71(3)	52(3)	63(3)	−16(3)	23(3)	−1(2)
T_2m	71(3)	59(3)	63(2)	−7(3)	25(3)	6(3)
O_A1	205(11)	108(9)	90(8)	−13(8)	85(8)	11(7)
O_A2	97(9)	63(8)	110(8)	−11(6)	28(7)	21(6)
O_B0	132(10)	132(9)	138(9)	−49(7)	80(8)	−28(7)
O_Bm	128(10)	145(9)	184(10)	12(7)	96(8)	−2(8)
O_C0	113(9)	98(9)	137(9)	−34(7)	50(8)	−10(7)
O_Cm	122(9)	83(8)	108(9)	4(7)	36(8)	−5(7)
O_D0	144(10)	105(9)	77(8)	2(7)	15(7)	4(7)
O_Dm	139(10)	121(9)	105(9)	−36(7)	−4(8)	0(7)
			Germanium albite ($NaAlGe_3O_8$)			
Na	163(8)	1234(22)	672(15)	176(11)	−51(9)	−726(16)
$T_1$0	80(2)	64(2)	68(2)	−8(1)	36(1)	2(1)
T_1m	84(2)	71(2)	66(2)	21(1)	31(2)	6(1)
$T_2$0	69(1)	48(1)	99(2)	0(1)	31(1)	4(1)
T_2m	78(1)	59(1)	96(1)	8(1)	33(1)	13(1)
O_A1	260(11)	109(9)	93(8)	27(8)	95(8)	18(7)
O_A2	72(8)	43(7)	148(9)	1(6)	22(7)	32(6)
O_B0	150(10)	121(9)	263(12)	−67(7)	145(9)	−67(8)
O_Bm	164(11)	280(13)	332(14)	62(9)	176(11)	22(10)
O_C0	131(9)	66(7)	193(10)	−22(6)	85(8)	−12(7)
O_Cm	137(9)	77(8)	151(9)	38(7)	4(7)	−7(7)
O_D0	143(9)	143(9)	103(9)	48(7)	9(7)	11(7)
O_Dm	191(11)	191(11)	133(10)	−35(8)	−23(8)	−10(8)

Note: Anisotropic temperature factors have the form $\exp[-\frac{1}{4}(B_{11}h^2a^{*2} + \ldots + 2B_{23}klb^*c^*\cos\alpha^*)]$.

$AlGeO_4$. The flux-nutrient mixture consisted of equimolar proportions of $NaAlGeO_4$ (as oxides and carbonate), $Na_2WO_4\cdot 2H_2O$ and V_2O_5. It was soaked in a Pt crucible with a well-fitting lid at 1300 °C for 12 h, and cooled from 1000 °C at 1 °C/h to 500 °C. The flux was removed by soaking in warm H_2O. The products were multiphase: $NaAlGe_3O_8$ was present as a few large crystals up to 2 mm in diameter and was characterized by TEM and semiquantitative electron microprobe analysis and single crystal and powder X-ray diffraction.

The crystal used for reflection intensities was reduced in size with a scalpel blade and 600 mesh abrasive paper. It was prismatic, with dimensions of 0.10 × 0.13 × 0.20 mm and a calculated volume of 2.54×10^{-3} mm³. Other experimental details differing from those for the gallium albite study were as follows. The unit-cell parameters [$a = 8.419(1)$, $b = 13.298(3)$, $c = 7.354(1)$ Å, $\alpha = 94.49(1)$, $\beta = 116.25(1)$, $\gamma = 90.88(2)°$, $V = 735.1$ Å³] were refined from 20 reflections in the 2θ range 49.8–57.9°. Intensity data were measured by θ-2θ scans with a scan angle (2θ) = 2.4°. A total of 6452 *hkl* reflections allowed by space group $C\bar{1}$ out to $2\theta = 70°$ were measured ($-14 \leq h \leq 14$, $-22 \leq k \leq 22$, $-12 \leq l \leq 12$). Standard reflections were 002, 130, −202. Transmission factors ($\mu = 131.0$ cm⁻¹) varied from 0.214 for 0,0,1 to 0.307 for 4,20,−1. There were 3226 unique reflections, with 929 considered unobserved.

Using all reflections out to $2\theta = 70°$ and 119 variable parameters, the structure refinement converged to $R = 0.026$, $R_w = 0.032$ [$S = 1.112$, $(\Delta/\sigma)_{max} = 5 \times 10^{-5}$, $\Delta\rho = -0.91$ eÅ^{-3} at 0.28,0.07,0.05 to 0.91 eÅ^{-3} at 0.29,0.04,0.11 (both near Na), $g = 1.30(4) \times 10^{-4}$]. Final parameters are given in Tables 1 and 2, and observed and calculated structure factors in Table 3.

DISCUSSION

Selected bond distances and bond angles for gallium albite and germanium albite are given in Tables 4 and 5, tetrahedral-site occupancies are given in Table 6, and the stereochemical environments of Na are represented in Figure 1.

Stoichiometry

Direct confirmation of the end-member compositions of gallium and germanium albite to within the precision normally expected of electron microprobe analysis of aluminosilicates is not possible without matching standards. However, both phases presently investigated are homogeneous by electron microprobe analysis, their unit-cell parameters are consistent with those of previous studies, and significant residual electron densities were not present at cation positions.

Tetrahedral site occupancies

The gallium albite sample investigated in this study has the expected low structure (cf. Swanson, 1986; Burns and Fleet, 1990), with Ga concentrated in the $T_1$0 site and minor, residual amounts of Ga in T_1m, $T_2$0, and T_2m (Table 6). This low gallium albite, which was annealed at 600 °C, is slightly more ordered than that of Swanson (1986), which was annealed at 650 °C. In most other respects the results of the two refinements (this study and Swanson) are very similar; interatomic distances and angles generally agree within a few standard deviations but there are minor discrepancies in thermal parameters. The gallium albite of this study is more ordered than the most ordered experimental product of Burns and Fleet (1990; sample Gb37, listed in Table 6), which was annealed at 672 °C. The higher t_1m value (0.11) in the latter may reflect a degree of imprecision in the Rietveld method but these numbers may not be directly comparable. For example, in Burns and Fleet (1990) the Rietveld method was used to analyze the bulk experimental product, whereas the present single crystal X-ray structure procedure was limited to just one crystal product of good diffraction quality. It is noted that the presence of intermediate gallium albite structure, within the range 913–937 °C, was established independently by Burns and Fleet (1990) by both Ga site occupancies from Rietveld powder X-ray diffraction refinement and unit-cell parameters.

As expected from the unit-cell parameters, the earlier powder diffraction work of Pentinghaus (1970), and the refinement of Grunwald (1981), the germanium albite sample is disordered (Table 6). However, it is not completely disordered, and the tetrahedral-site ordering pattern, with $t_1m > t_10 \approx 0.25$, is apparently unique. This result is consistent with the qualitative inference of Smith and Brown (1988), but the present values on mean T-O distances (Table 4; see below) and tetrahedral-site occupancies (Table 6) do not support depletion of Al in T_20. In summary, the present germanium albite appears to have an unusual intermediate structure.

Atomic substitution and tetrahedral-site ordering

In principle, details of the alkali feldspar structure depend on substitution of both large nonframework cations (Na, K, Rb, Cs, Ca, Ba . . .) and tetrahedral-site atoms (Si, Al, Fe^{3+}, Ga, Ge, B . . .). However, qualitative comparisons of galliosilicate, alumino-germanate, aluminosilicate, and boro-silicate sodium feldspar structures reveal broad similarities in positional and thermal parameters, stereochemistries of Na and tetrahedral-site atoms, T-O-T bond angles (Table 5), and so on. Clearly, the major changes in sodium feldspar structures, compared to those of potassium feldspar, result from accommodation of the smaller-sized Na cation. The feldspar framework accommodates large cations like K with little distortion, contributing to the extensive temperature stability of the monoclinic structure in potassium feldspars.

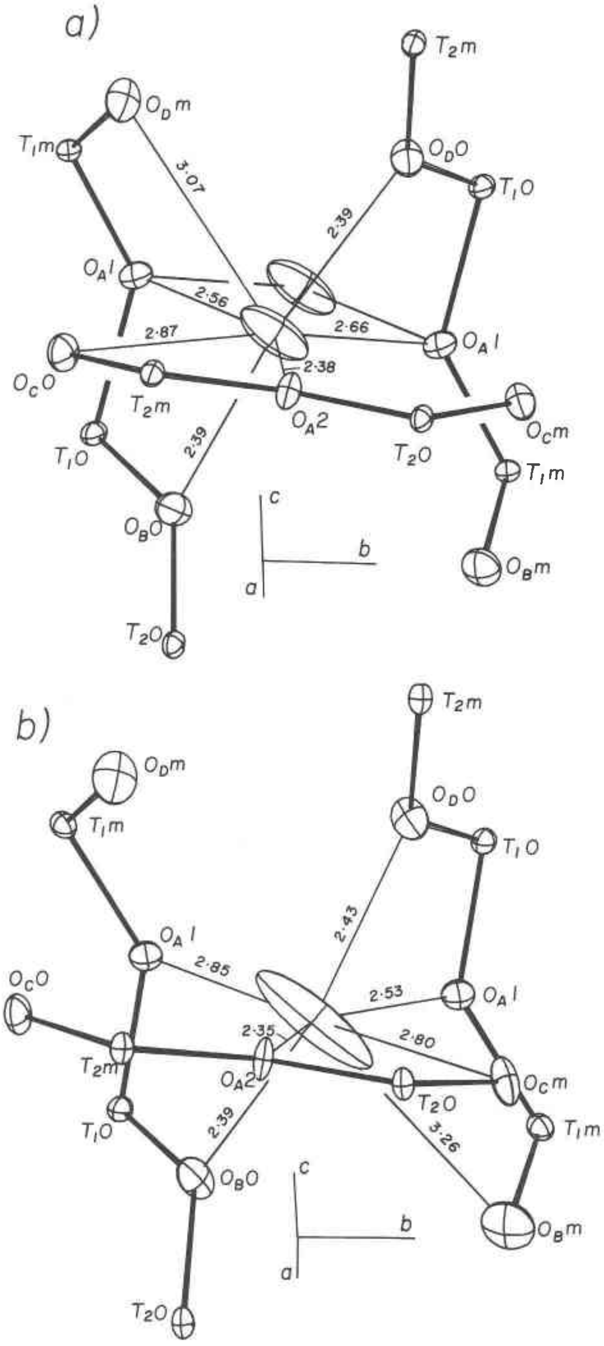

Fig. 1. Stereochemical environment of Na (at 0.3,0.0,0.1) to 4 Å: (**a**) low gallium albite (second Na atom in sphere is at −0.3,0.0,−0.1); (**b**) intermediate germanium albite: bond distances are Å.

To accommodate the smaller Na cation in the feldspar framework, O atoms O_A2, O_B0, and O_D0 move closer to the nonframework cation, decreasing the corresponding T-O-T bond angles and forming three short coplanar bonds with Na. In addition, two short-to-medium Na-O bonds are formed with O_A1 O atoms in low albite and low gallium albite; in intermediate germanium albite these bonds are modified to one short-to-medium Na-O_A1 bond, lying close to the plane of strongest Na-O bonding, and one long Na-O_A1 distance. Whereas the T-O_B0-T and T-O_D0-T angles decrease with Na substitution, the corresponding angles related by the symmetry plane in the monoclinic space group (at O_Bm and O_Dm) increase (Table 5). Thus, crimping of the framework at O_B0 and O_D0 is compensated by stretching at O_Bm and O_Dm; this coupled distortion is the principal cause for the increase in

TABLE 4. Selected interatomic distances (Å) and bond angles (°)

	$NaGaSi_3O_8$	$NaAlGe_3O_8$		$NaGaSi_3O_8$	$NaAlGe_3O_8$
Na-O_A1	2.655(3)	2.529(4)	Na-O_Bm	—	3.264(5)
Na-O_A1	2.555(3)	2.853(4)	Na-O_C0	2.871(3)	—
Na-O_A2	2.377(3)	2.348(3)	Na-O_Cm	—	2.804(4)
Na-O_B0	2.394(2)	2.392(3)	Na-O_Dm	3.065(3)	—
Na-O_D0	2.392(3)	2.433(3)			
$T_1$0-O_A1	1.815(2)	1.728(2)	$T_2$0-O_A2	1.640(2)	1.760(2)
$T_1$0-O_B0	1.808(2)	1.738(2)	$T_2$0-O_B0	1.597(2)	1.750(2)
$T_1$0-O_C0	1.795(2)	1.734(2)	$T_2$0-O_Cm	1.608(2)	1.729(2)
$T_1$0-O_D0	1.808(2)	1.746(2)	$T_2$0-O_Dm	1.614(2)	1.704(3)
average	1.807	1.737	average	1.615	1.736
T_1m-O_A1	1.597(2)	1.741(2)	T_2m-O_A2	1.644(2)	1.747(2)
T_1m-O_Bm	1.600(2)	1.718(3)	T_2m-O_Bm	1.616(2)	1.706(3)
T_1m-O_Cm	1.621(2)	1.737(2)	T_2m-O_C0	1.606(2)	1.743(2)
T_1m-O_Dm	1.622(2)	1.717(3)	T_2m-O_D0	1.610(2)	1.743(2)
average	1.610	1.728	average	1.619	1.735
O_A1-$T_1$0-O_B0	101.0(1)	102.6(1)	O_A2-$T_2$0-O_B0	109.9(1)	105.8(1)
O_A1-$T_1$0-O_C0	118.8(1)	118.4(1)	O_A2-$T_2$0-O_Cm	104.7(1)	102.0(1)
O_A1-$T_1$0-O_D0	101.7(1)	102.6(1)	O_A2-$T_2$0-O_Dm	107.6(1)	108.9(1)
O_Bm-$T_1$0-O_C0	112.1(1)	109.0(1)	O_B0-$T_2$0-O_Cm	112.0(1)	112.2(1)
O_Bm-$T_1$0-O_D0	110.6(1)	112.4(1)	O_B0-$T_2$0-O_Dm	111.6(1)	113.0(1)
O_Cm-$T_1$0-O_D0	111.8(1)	111.5(1)	O_C0-$T_2$0-O_Dm	110.7(1)	113.9(1)
O_A1-T_1m-O_Bm	109.8(1)	105.2(1)	O_A2-T_2m-O_Bm	109.2(1)	112.6(1)
O_A1-T_1m-O_Cm	112.7(1)	112.3(1)	O_A2-T_2m-O_C0	104.6(1)	105.5(1)
O_A1-T_1m-O_Dm	107.2(1)	105.0(1)	O_A2-T_2m-O_D0	108.0(1)	107.2(1)
O_Bm-T_1m-O_Cm	108.4(1)	108.9(1)	O_Bm-T_2m-O_C0	110.3(1)	108.8(1)
O_Bm-T_1m-O_Dm	110.8(1)	115.1(2)	O_Bm-T_2m-O_D0	110.5(1)	112.0(1)
O_Cm-T_1m-O_Dm	108.1(1)	110.2(1)	O_C0-T_2m-O_D0	113.9(1)	110.6(1)

the interaxial angle α (to about 94°). Substitution by a larger tetrahedral-site atom (Ga, Ge) results principally in increase in T-O bond lengths which is compensated for by a tendency for decrease in the T-O-T bond angles of O atoms more strongly bonded to Na. Correspondingly, substitution by a smaller tetrahedral-site atom (B) causes these T-O-T angles to increase (Table 5).

The position of the Na cation does not permit complete local charge balancing of O atoms (i.e., charge balancing within the first coordination sphere). In particular, O_A2, which is coordinated to $T_2$0, T_2m, and Na (Fig. 1), is markedly overbonded in low albites, as determined using valence summation procedures. The equivalent feature is present in the monoclinic potassium feldspar structure (e.g., Prince et al., 1973). However, the persistence of local charge (or valence electron) imbalance in ordered structures, with valence requirements being satisfied over an extended sphere, does tend to minimize the importance of covalence effects alone in controlling ordering on tetrahedral sites. Space-fitting requirements of substituents (with the necessary adjustments in bond distances, bond strengths, bond angles, etc.) must be at least a contributing factor.

The overall control on tetrahedral-site ordering in alkali feldspars and the interrelationships between ordering, stereochemistry, and bonding effects remain controversial (e.g., Smith, 1974; Smith et al., 1986). Final resolution of these complex problems awaits the development of appropriate numerical models for energy minimization (cf. Post and Burnham, 1987). In the interim, study of the response of the alkali feldspar structure to selected substituents may provide a basis for testing hypotheses and critical concepts.

One correlation in silicates which has been discussed extensively is that between tetrahedral site occupancies and mean T-O-T angles (Brown and Gibbs, 1970; Liebau, 1985). The mean T-O-T bond angle, number of O atoms associated with short Na-O distances, and mean Si-O bond length for the tetrahedral sites in low gallium albite are, respectively; $T_1$0 (132.5°, 3, Al-O), T_1m (148.2°, 1, 1.610 Å), $T_2$0 (139.6°, 2, 1.615 Å), and T_2m (137.4°, 2, 1.619 Å). Very similar values are found in the low albite structure. Mean T-O-T bond angle and Si-O bond length clearly correlate with proximity of O atoms to the Na cation. But does the observed ordering scheme result because the valence requirements of Al are balanced more efficiently in the $T_1$0 site or because Si can form π bonds with O atoms in the T_1m, $T_2$0, and T_2m sites?

Future study of binary (and more complex) analogue

TABLE 5. O (T-O-T) bond angles in gallium and germanium albite and other alkali feldspars

	Gallium albite	Germanium albite	Low albite	Reedmergnerite	Intermediate Albite	Intermediate Microcline
$T_1$0-O_A1-T_1m	137.9(1)	139.5(1)	141.5	143.1	142.7	144.3
$T_2$0-O_A2-T_2m	130.7(1)	125.2(1)	129.7	128.7	129.8	138.8
$T_1$0-O_B0-$T_2$0	134.9(1)	132.8(1)	139.8	140.5	140.4	152.8
T_1m-O_Bm-T_2m	161.9(2)	157.0(2)	161.5	158.1	159.4	152.8
$T_1$0-O_C0-T_2m	125.2(1)	124.4(1)	129.8	124.9	130.3	131.1
T_1m-O_Cm-$T_2$0	138.1(1)	131.3(1)	135.8	135.9	134.7	131.1
$T_1$0-O_D0-T_2m	131.8(1)	130.8(1)	133.9	135.4	134.9	141.4
T_1m-O_Dm-$T_2$0	154.7(2)	150.0(2)	151.8	146.3	150.5	141.7

Note: Low albite—Harlow and Brown (1980); reedmergnerite—Appleman and Clark (1965); intermediate albite—Phillips et al. (1989); intermediate microcline—Dal Negro et al. (1978).

TABLE 6. Tetrahedral-site occupancies of Ga and Al in some alkali feldspars

	Reference	$t_1$0	t_1m	$t_2$0	t_2m
Gallium albite	1	0.935(1)	0.016(1)	0.025(1)	0.025(1)
Gallium albite	2	0.887	0.031	0.044	0.038
Gallium albite	3	0.85	0.11	0.03	0.00
Low albite	4	0.97	0.04	0.0	0.0
Germanium albite	1	0.274(2)	0.375(2)	0.185(2)	0.166(2)
High albite	5	0.28	0.25	0.22	0.25
Intermediate albite	6	0.510	0.155	0.164	0.171
Low sanidine	7	0.345		0.125	
Intermediate microcline	8a	0.370	0.350	0.150	0.140
Intermediate microcline	8b	0.445	0.330	0.085	0.080
Intermediate microcline	9	0.63	0.235	0.045	0.03

Note: References: 1 = present study; 2 = Swanson (1986); 3 = Bruns and Fleet (1990); 4 = Harlow and Brown (1980); 5 = Ribbe et al. (1969); 6 = Phillips et al. (1989); 7 = Colville and Ribbe (1968); 8 = Dal Negro et al. (1978; a is P2B, b is P17C); 9 = Bailey (1969).

compositions and of structures of intermediate states of order will provide independent assessment of the preference of trivalent atoms for the $T_1$0 site. For example, in incipiently disordered Amelia albite, Fe^{3+} (in minor amounts) is restricted to the $T_1$0 site and does not participate in exchange of Al and Si on the other tetrahedral sites (Petrov et al., 1989). This suggests that the ordering scheme is determined by preference of the trivalent atoms for the $T_1$0 site.

As reviewed by Smith (1974), in monoclinic potassium feldspar ($t_1 > t_2$) the coordination of O_A1 to two K cations may facilitate a favorable distribution of charge when Al is placed in the T_1 site. Moreover, this completes a four-coordinated (nearly tetrahedral) environment for O_A1, which would correspond to hybridized sp^3 orbitals on the O atom. Regardless of the precise role of O_A1, it is considered significant that the stereochemical relationship between the nonframework cation and T_1-site atom in the monoclinic feldspar is conserved for $T_1$0 in low albite and low gallium albite but not for T_1m.

The preference of trivalent substituents for the $T_1$0 site of sodium feldspar appears to decrease in the sequence $Fe^{3+} > Ga > B > Al$. Ordering of B and Si invariably occurs in borosilicates and, therefore, B should have a greater preference than Al for the $T_1$0 site. Also, B and Si are completely ordered in reedmergnerite (Appleman and Clark, 1965), and $NaBSi_3O_8$ disorders at a lower temperature than $NaGaSi_3O_8$ (<700 °C, Bruno and Pentinghaus, 1974, and 890–970 °C, Burns and Fleet, 1990, respectively). This preference sequence correlates with decrease in the difference between the radius of a cation and that of Si [Fe^{3+} (0.23), Ga (0.21), B (0.15), Al (0.13 Å); data from Shannon, 1976], but not with either electronegativity or bond strength.

An additional effect contributing to tetrahedral site preference in alkali feldspars may be electrostatic repulsion between the tetrahedral atoms and alkali metal (M) across shared coordination edges (cf. Fleet, 1974). This destabilization will increase with increase in valence of the tetrahedral atom and electronegativity difference with O, and decrease in T-M distance. In low gallium albite the average T-Na distances within the Na sphere to 4 Å are $T_1$0 (3.20), T_1m (3.58), $T_2$0 (3.56), and T_2m (3.45 Å); clearly, if Si occupied the $T_1$0 site, the average $T_1$0-Na distance would be significantly smaller than 3.20 Å. Thus, electrostatic repulsion is minimized with Si in the T_1m, $T_2$0, and T_2m sites and Ga in $T_1$0. In low gallium albite and low albite the T_1m site is stereochemically distinct from the $T_2$0 and T_2m sites in that its first coordination sphere includes the O atom O_A1, which is closely associated with two Na atoms (Fig. 1a). Hence, the site preference by Si should be selective. The presently available results for albite and gallium albite suggest otherwise. Burns and Fleet (1990), however, did observe a tendency for $t_2$0 to behave independently of t_2m (Fig. 1a).

The weak preference of Al for the T_1m site in intermediate germanium albite (Table 6) is unexplained. Ge and Al have very similar mean atomic radii in tetrahedral coordination with O (0.390 and 0.39 Å, respectively, in Shannon, 1976). For example, Klaska (1974) obtained mean Ge-O and Al-O bond distances of 1.746 and 1.747 Å, respectively, in $NaAlGeO_4$ (beryllonite structure). However, well-refined structures of sodium aluminogermanate sodalite [$(Na_8Al_6Ge_6O_{24})A_2$; Fleet, 1989] yielded consistently larger values for mean Al-O bond distances; Ge-O and Al-O bond distances were found to be, respectively, 1.740 and 1.743 Å for A = Cl, 1.737 and 1.745 Å for A = Br, and 1.734 and 1.745 Å for A = I. In suggesting that Al favored T_1m, Smith and Brown (1988) assumed Al to have a smaller radius than Ge in germanium albite. Although T_1m does have the highest Al occupancy (0.375) and the smallest average T-O distance (1.728 Å), the latter may be attributable to stereochemical environment; i.e., as noted above, T_1m has the fewest O atoms associated with short Na-O distances and greatest average T-O-T angle. More generally, T_1m has the smallest average T-O distances in low albite, low gallium albite, and reedmergnerite. Compared to trends for average T-O distances in most alkali feldspar structures, including those of the present study, the value of 1.756 Å reported by Grunwald (1981) for $T_2$0 in germanium albite is anomalously high. Average T-Na distances in germanium albite are $T_1$0 (3.24), T_1m (3.60), $T_2$0 (3.45), and T_2m (3.77 Å). Thus, on the basis of local charge (or valence) balance, atomic size difference, and electrostatic repulsion, Al should have a similar but diminished site preference in intermediate germanium albite compared to that in low albite or low gallium albite. However, the overall similarity in atomic size of Ge and Al (which differ markedly in electronegativity) readily explains the existence of the disordered aluminogermanate feldspar structure at low temperatures. Moreover, the total t_1 and t_2 occupancies in intermediate germanium albite [$(t_10 + t_1m) = 0.649$, $(t_20 + t_2m) = 0.351$] are similar to those in low sanidine and some intermediate microcline.

In summary, tetrahedral site ordering in strain-free sodium silicate feldspar structures is promoted by the distinctive stereochemistries of the T_10 and T_1m sites, which are imposed by spatial accommodation of the Na cation within the feldspar framework. It is tentatively concluded that the ordering scheme is determined by the favorable charge or valence electron distribution resulting when the trivalent atom occupies the T_10 site, and that this site preference is proportional to difference in size with the quadrivalent atom. Electrostatic repulsion between the tetrahedral-site atoms and Na may be a contributing factor.

Na atom position

The Na atom in albite structures is relatively unconstrained transverse to the plane of the strongest Na-O bonds. Therefore, thermal vibration in this tranverse direction is exaggerated. The Na atom position in sodium enneagermanate ($Na_4Ge_9O_{20}$, Fleet, 1990) has an analogous stereochemistry and its vibrational ellipsoid is similarly markedly anisotropic transverse to the plane of strongest Na-O bonds. Additionally, the Na atom in albite may experience static displacement along the major axis of the vibrational ellipsoid, stretching the stronger Na-O bonds only marginally and forming shorter bonds with other proximal O atoms. Such cation positions may represent positions of lower potential energy, particularly in disordered structures.

Further refinement of the low gallium albite structure with two half-atom positions for Na failed to converge. Also, further refinement of the intermediate germanium albite structure with four quarter-atom positions for Na was slow to converge and did not appear to be significant ($R = 0.025$, $R_w = 0.029$).

The studies of Winter et al. (1977), Harlow and Brown (1980), and Swanson (1986) all favor a single atom position with markedly anisotropic thermal motion for Na in low albite and low gallium albite. It is unlikely that a split-atom position, corresponding to two minima in potential energy, would exist in ideally ordered low albite. However, the mobility of alkali metals in framework structures with large cavities is well known. Thus, small fluctuations of electrical potential in low albite crystals, caused by crystal defects, might be sufficient to effect local displacements of the Na atom. Such displacements would still be present at 0 K and might explain the zero-point energy reported by Smith et al. (1986).

It seems most probable that local displacements of the Na atom do occur in disordered (high) albite structures, promoted by tetrahedral-site disorder and crystal defects. The electron density distribution at the Na position in intermediate germanium albite (e.g., Fig. 1b) is quite comparable to that in high albite at room temperature (Prewitt et al., 1976; Winter et al., 1977), and therefore favors local static displacement. However, there does not appear to be any basis for specifying four quarter-atom positions for Na. There would surely be a multiplicity of local positions for Na in a disordered framework, as in the structure-energy calculations of Post and Burnham (1987). It is noteworthy that, from comparison of thermal parameters in intermediate germanium albite and low gallium albite, the corresponding displacements in the alkali feldspar framework itself are rather small. As expected, for both of the present structures, thermal anisotropy of O atoms is greatest transverse to the bonding plane, and the overall isotropic thermal motion is least for O_A2, which is firmly bonded to the Na atom.

As noted in Fleet (1990), there is good correlation between size of thermal ellipsoid and structural topology. In $(Ni,Mg)_{10}Ge_3O_{16}$ (Fleet and Barbier, 1989), which has a closest-packed structure, the isotropic thermal parameters for Ge and O are 0.21–0.22 Å^2 and 0.38–0.42 Å^2, respectively. In open framework structures vibrational amplitudes are increased by anisotropic distribution of bonding forces and concerted motion. These effects appear to be somewhat more marked in alkali feldspars than in sodalite (Fleet, 1989).

ACKNOWLEDGMENTS

I thank G.E. Harlow for a constructive review of an earlier version of the manuscript, M. Arima for preparation of the single crystal of germanium albite, J. Barbier for TEM analysis, and the Natural Sciences and Engineering Research Council of Canada for financial support.

REFERENCES CITED

Appleman, D.E., and Clark, J.R. (1965) Crystal structure of reedmergnerite, a boron albite, and its relation to feldspar crystal chemistry. American Mineralogist, 50, 1827–1850.

Bailey, S.W. (1969) Refinement of an intermediate microcline structure. American Mineralogist, 54, 1540–1545.

Brown, G.E., and Gibbs, G.V. (1970) Stereochemistry and ordering in the tetrahedral portion of silicates. American Mineralogist, 55, 1587–1607.

Bruno, E., and Pentinghaus, H. (1974) Substitution of cations in natural and synthetic feldspars. In W.S. MacKenzie and J. Zussman, Eds., The feldspars, p. 574–609. Proceedings of NATO Advanced Study Institute, University Press, Manchester, England.

Burns, P.C., and Fleet, M.E. (1990) Unit-cell dimensions and tetrahedral-site ordering in synthetic gallium albite ($NaGaSi_3O_8$). Physics and Chemistry of Minerals, 17, 108–116.

Colville, A.A., and Ribbe, P.H. (1968) The crystal structure of an adularia and a refinement of the structure of orthoclase. American Mineralogist, 53, 25–37.

Coppens, P., and Hamilton, W.C. (1970) Anisotropic extinction corrections in the Zachariasen approximation. Acta Crystallographica, A26, 71–83.

Dal Negro, A., De Pieri, R., and Quareni, S. (1978) The crystral structures of nine K feldspars from the Adamello Massif (Northern Italy). Acta Crystallographica, B34, 2699–2707.

Fleet, M.E. (1974) Distortions in the coordination polyhedra of M site atoms in olivines, clinopyroxenes and amphiboles. American Mineralogist, 59, 1083–1093.

Fleet, M.E. (1989) Structures of sodium alumino-germanate sodalites [$Na_8(Al_6Ge_6O_{24})A_2$,A = Cl,Br,I]. Acta Crystallographica, C45, 843–847.

Fleet, M.E. (1990) Refinement of the structure of sodium enneagermanate ($Na_4Ge_9O_{20}$). Acta Crystallographica, C46, 1202–1204.

Fleet, M.E., and Barbier, J. (1989) Structure of aerugite ($Ni_{8.5}As_3O_{16}$) and interrelated arsenate and germanate structural series. Acta Crystallographica, B45, 201–205.

Grunwald, A. (1981) Die Anisotropie des Natriums und die Verteilung von Aluminium und Germanium im synthetischen Feldspat $NaAlGe_3O_8$. Diplomarbeit, Westfalischen Wilhelms-Universitat Munster.

Harlow, G.E., and Brown, G.E., Jr. (1980) Low albite: An X-ray and neutron diffraction study. American Mineralogist, 65, 986–995.

International tables for X-ray crystallography, vol. IV. (1974) Kynoch Press, Birmingham, England.

Klaska, K.-H. (1974) Strukturuntersuchungen an Tridymitabkommlingen (Beryllonitreihe, Trinephelin), dissertation, University of Hamburg, Hamburg.

Kroll, H., and Ribbe, P.H. (1983) Lattice parameters, composition and Al,Si order in alkali feldspars. In Mineralogical Society of America Reviews in Mineralogy, 57–99.

Kroll, H., and Ribbe, P.H. (1987) Determining (Al,Si) distribution and strain in alkali feldspars using lattice parameters and diffraction-peak positions: A review. American Mineralogist, 72, 491–506.

Liebau, F. (1985) Structural chemistry of silicates. Springer-Verlag, Berlin.

Pentinghaus, H. (1970) Der Einbau von Al(III), Ga(III), Fe(III) und Si(IV), Ge(IV) in synthetische Alkalifeldspäte. Dissertation, University of Münster, Münster, Germany.

Petrov, I., Yude, F., Bershov, L.V., Hafner, S.S., and Kroll, H. (1989) Order-disorder of Fe^{3+} ions over the tetrahedral positions in albite. American Mineralogist, 74, 604–609.

Phillips, M.W., Ribbe, P.H., and Pinkerton, A.A. (1989) Structure of intermediate albite, $NaAlSi_3O_8$. Acta Crystallographica, C45, 542–545.

Post, J.E., and Burnham, C.W. (1987) Structure-energy calculations on low and high albite. American Mineralogist, 72, 507–514.

Prewitt, C.T., Sueno, S., and Papike, J.J. (1976) The crystal structure of high albite and monalbite at high temperatures. American Mineralogist, 61, 1213–1225.

Prince, E., Donnay, G., and Martin, R.F. (1973) Neutron diffraction refinement of an ordered orthoclase structure. American Mineralogist, 58, 500–507.

Ribbe, P.H. (1983) Mineralogical Society of America Reviews in Mineralogy, 2.

Ribbe, P.H., Megaw, H.D., Taylor, W.H., Ferguson, R.B., and Traill, R.J. (1969) The albite structures. Acta Crystallographica, B25, 1503–1518.

Shannon, R.D. (1976) Revised effective ionic radii and systematic studies of interatomic distances in halides and chalcogenides. Acta Crystallographica, A32, 751–767.

Smith, J.V. (1974) Feldspar minerals, vol. 1. Springer-Verlag, Berlin.

Smith, J.V., and Brown, W.L. (1988) Feldspar Minerals, vol. 1, (2nd edition). Springer-Verlag, Berlin.

Smith, J.V., Artioli, G., and Kvick, A. (1986) Low albite, $NaAlSi_3O_8$: Neutron diffraction study of crystal structure at 13 K. American Mineralogist, 71, 727–733.

Su, S.-C., Ribbe, P.H., Bloss, D., and Goldsmith, J.R. (1986) Optical properties of single crystals in the order-disorder series low albite-high albite. American Mineralogist, 71, 1384–1392.

Swanson, D.K. (1986) High-temperature crystal chemical formalisms applied to $K_2Si^{VI}Si_3{}^{IV}O_9$ and $NaGaSi_3O_8$. Ph.D. thesis, State University of New York, Stony Brook.

Wainwright, J.E., and Starkey, J. (1968) Crystal structure of a metamorphic low albite. Geological Society of America Meeting, Mexico City, Abstracts with Programs, 310.

Winter, J.K., Ghose, S., and Okamura, F.P. (1977) A high-temperature study of the thermal expansion and the anisotropy of the sodium atom in low albite. American Mineralogist, 62, 921–931.

MANUSCRIPT RECEIVED FEBRUARY 14, 1990
MANUSCRIPT ACCEPTED NOVEMBER 10, 1990